Vortex excitations in the insulating state of an oxide interface

M. Mograbi,[1] E. Maniv,[1] P. K. Rout,[1] D. Graf,[2] J.-H. Park,[2] and Y. Dagan[1]
[1]*Raymond and Beverly Sackler School of Physics and Astronomy, Tel-Aviv University, Tel Aviv, 69978, Israel*
[2]*National High Magnetic Field Laboratory, Tallahassee, Florida 32310, USA*

(Received 9 March 2018; revised manuscript received 28 November 2018; published 11 March 2019)

In two-dimensional (2D) superconductors, an insulating state can be induced either by increasing disorder or by applying a magnetic field H. Many scenarios have been put forth to explain the superconductor to insulator transition (SIT). One of the main difficulties in discerning between the various scenarios is to elucidate the nature of the emergent insulating state. This complicatedness stems from the lack of a continuous mapping of the superconducting to insulating phase diagram in a single sample. Here we use the 2D electron liquid formed at the interface between (111) $SrTiO_3$ and $LaAlO_3$ to study the SIT as a function of electrostatic gate and magnetic field. This crystalline interface exhibits very prominent features: (a) a very large and anisotropic magnetoresistance (MR) peak emerging from the superconducting state and persisting even when the sample is totally insulating, (b) hysteresis in the MR peak, and (c) linear MR for low perpendicular magnetic fields. We identify a new magnetic field scale, where the superconducting fluctuations are muted, and find a length scale ξ_{ins} for the vortex fluctuation in the insulating state. Our findings suggest that vortex excitations and Cooper pair localization are responsible for the observed SIT. Surprisingly, these excitations exist even when the sample is tuned into the zero-field insulating state.

DOI: 10.1103/PhysRevB.99.094507

I. INTRODUCTION

The nature of the quantum phase transition where the ground state of a 2D system transitions from a superconductor into an insulator upon changing a control parameter such as disorder or magnetic field is still under debate. The SIT has been demonstrated in various systems such as Bi [1], InO_x [2–7], TiN_x [8,9], MoGe [10], cuprate superconductors [11,12], oxide interfaces [13–15], and more [16–21].

The scenarios put forth to explain the SIT can be roughly divided into two main categories. The fermionic scenarios suggest the insulating behavior is the result of fermionic physics dominating after the breaking of Cooper pairs [22–24], whereas in the bosonic scenarios the insulating state is related to the existence of Cooper pairs. The two main theoretical ideas for the bosonic insulator are loss of phase coherence between superconducting islands embedded in an insulating matrix [25–28] and localization of Cooper pairs with concomitant condensation of vortex excitations [29,30].

The many features observed in the SIT, such as scaling near a quantum critical point [2,3,5,10–12,17], large magnetoresistance (MR) peaks [5–9,21], and thermally activated insulating behavior [6–8,19], are not necessarily observed in all materials that undergo a SIT. Owing to the fact that changing tuning parameters sometimes requires changing of the sample itself, continuous tuning from the superconductor to the insulating state in a single sample is still lacking. These issues render the interpretation of various phenomena difficult and the mechanism behind the SIT debateable.

In this paper we study the SIT phase diagram of the (111) oriented interface between the two band insulators $LaAlO_3$ and $SrTiO_3$. The interface has a gate tunable carrier density and it can form on the various faces of the $SrTiO_3$ crystal: (100), (110), and (111) [31]. While for (100) the cubic symmetry is projected onto the interface and creating a square lattice, the (111) oriented $LaAlO_3/SrTiO_3$ interface has a 2D triangular structure. This 2D crystalline symmetry is also reflected in the magnetotransport properties [32]. Previous studies of this system found 2D superconductivity [33,34] and a correlation between superconductivity and spin-orbit interaction [35]. While SITs have been reported in the (100) [13,15] and (110) [14] interfaces, they present a significantly weaker insulating behavior compared to the (111) interface. The idea of charge-vortex duality has been demonstrated in (100) interface where ferromagnetic response has also been reported [36].

We use gate bias to tune the sample from the metallic and superconducting regime to the insulating regime. At various gate voltages we study the magnetic field response for parallel and perpendicular field orientations. We observe giant magnetoresistance features similar to those observed in amorphous 2D superconductors [5–9] previously unseen in a crystalline material. From the comparison between the effects of parallel and perpendicular magnetic fields we define an energy scale for the suppression of the insulating state via the breaking of Cooper pairs. This anisotropic magnetoresistance as well as the linear magnetoresistance observed at low fields (and the resulting length scale) along with the hysteresis of the magnetoresistance features show that vortex excitations are responsible for the SIT. Surprisingly, these effects persist deep into the insulating state, revealing the importance of vortex excitations even when superconductivity is completely suppressed.

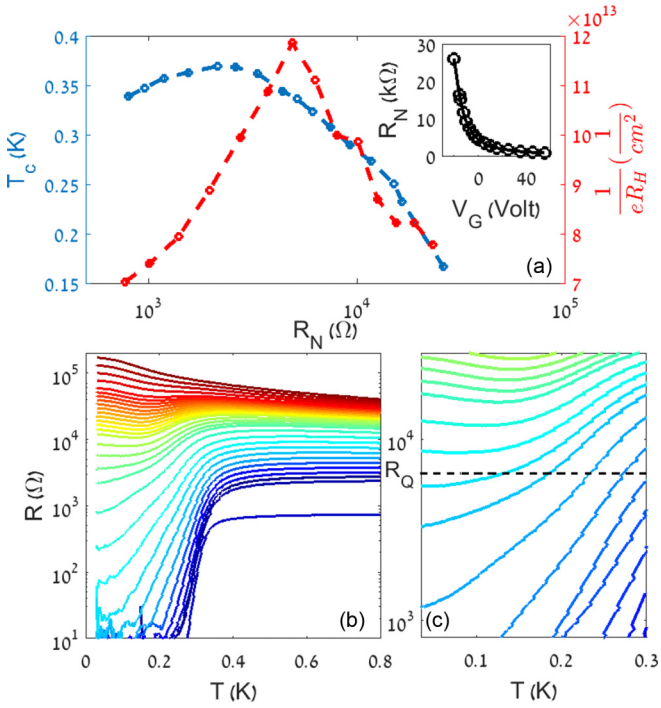

FIG. 1. (a) Superconducting critical temperature T_c and inverse hall coefficient $\frac{1}{eR_H}$ measured at 2 K as a function of normal state sheet resistance R_N. The inset shows R_N vs V_g at 2 K. (b) Sheet resistance R_S (in log scale) against T for V_g ranging from 30 (dark blue) to −190 V (dark red). (c) R_S plotted against T for those same voltages near the critical point, where $\frac{dR_S}{dT}_{T\to 0} = 0$. The black dashed line indicates the value of the quantum resistance $R_Q = \frac{h}{4e^2}$.

II. METHODS

Epitaxial films of $LaAlO_3$ were deposited on atomically flat $SrTiO_3$ (111) substrate using pulsed laser deposition. The details of deposition procedure and substrate treatment are described in Refs. [32,35]. We monitor the layer-by-layer growth of 14 monolayers (LaO_3/Al layers) by reflection high energy electron diffraction (RHEED) oscillations (see the Supplemental Material for more details [37]). Atomic force microscope images show the step and terrace morphology of the film with step heights of 0.22 nm. A gold back-gate electrode is evaporated on the bottom of the $SrTiO_3$ crystal. The positive voltage terminal is connected to the bottom gate electrode. The data presented in the paper were collected for sample B7, measured in the van der Pauw method. Several samples exhibited similar behaviors and their measurements are presented in the Supplemental Material [37]. The measurements presented in Figs. 1 and 2 were conducted with a Keithley 6221 current source and Keithhley 2182A nanovoltmeter in a delta mode configuration inside an Oxford Instruments Triton 400 dilution refrigerator (with a base temperature of ∼30 mK). The measurements in Figs. 3, 4(a), and 4(b) were measured with a Lakeshore 372 resistance bridge in a wet dilution refrigerator at the National High Magnetic Field Laboratory (NHMFL) in Tallahassee (with a base temperature of ∼20 mK). Hall measurements were performed in a He^4 cryostat at a temperature of 1.5 K with a Keithley 6221 current source and Keithhley 2182A nanovoltmeter in a delta mode configuration. IV measurements were taken in order to ensure the currents used in resistance measurements are in the linear response regime. The currents used were between 1×10^{-10} and 1×10^{-8} A.

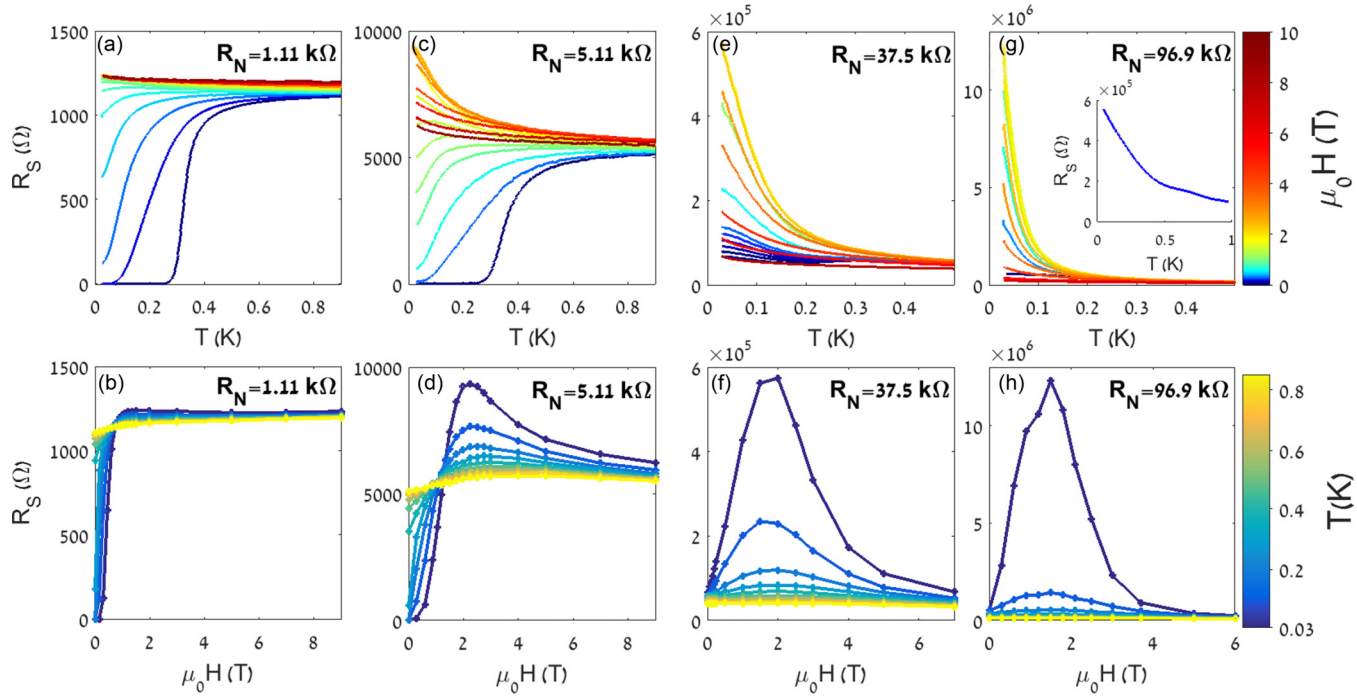

FIG. 2. (a), (c), (e), and (g) $R_S(T)$ for perpendicular magnetic field (H) ranging from 0 (dark blue) to 9 T (dark red) for four different R_N. The inset of (g) shows the zero field $R_S(T)$ for $R_N = 96.9$ kΩ, exhibiting insulator-type behavior down to base temperature. (b), (d), (f), and (h) $R_S(H)$ at different T ranging from 0.035 (dark blue) to 0.85 K (yellow) for the same R_N.

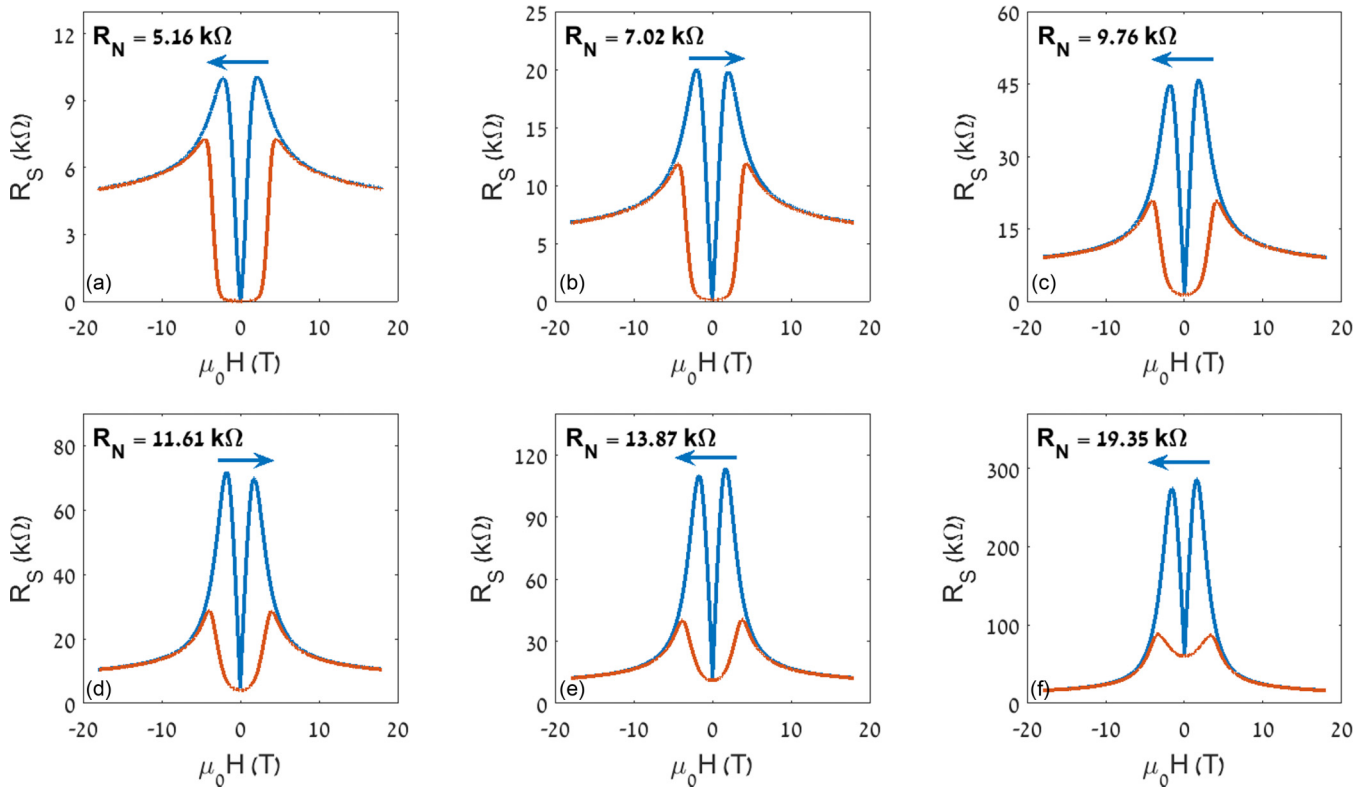

FIG. 3. MR at 21 mK plotted for magnetic fields perpendicular (blue) and parallel (red) to the sample surface for different R_N. The small asymmetry in MR peaks for perpendicular field is related to the sweep direction (blue arrows).

III. EFFECT OF ELECTROSTATIC GATING

The large dielectric constant ϵ of $SrTiO_3$ ($\approx 20000\epsilon_0$) allows strong modulation of the carrier density at the interface with back-gate voltage (V_g) [38]. The inset of Fig. 1(a) shows the normal state sheet resistance R_N as a function of V_g. While the overall behavior is reproducible, the exact values of V_g can shift for different cool downs (see the Supplemental Material for more information [37]). This can be due to different domain configuration [39,40] and trapped charges [41]. We therefore use R_N rather than V_g as our reproducible tuning parameter in the phase diagram.

The behavior of the superconducting transition temperature T_c and the low-field inverse Hall coefficient $\frac{1}{eR_H}$ for low R_N (or high V_g) [Fig. 1(a)] is consistent with Refs. [35,42,43]. At high

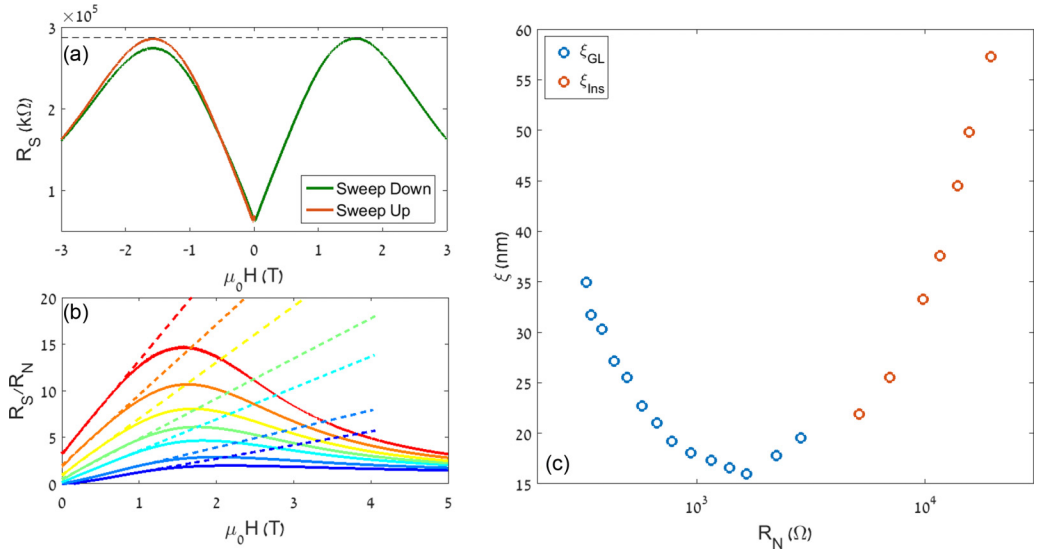

FIG. 4. (a) MR at 21 mK for up (red) and down (green) field sweeps. (b) R_S/R_N at 21 mK as a function of magnetic field for R_N ranging from 5.16 (blue) to 19.35 kΩ (red). The dashed lines show low-field regions fits to the flux-flow behavior: $R_S/R_N \propto H$. (c) The coherence length as calculated from the perpendicular critical field [35] (blue) and the slope of low-field MR (red) as a function of R_N.

R_N the effect of V_g on $\frac{1}{eR_H}$ reverses. This unusual behavior has been attributed to the electron and hole contributions arising from highly curved Fermi contours of a sixfold symmetric interface [43] in addition to electronic correlations similar to the (100) interface [44].

The observed change in carrier density cannot explain the strong gate response of R_N, implying that the mobility is the dominant factor, similarly to what was suggested for the (100) interface [45]. The effect of V_g on superconductivity is therefore twofold: First, it changes electron density and hence superfluid stiffness. Second, it modifies the effective disorder, possibly by bringing the electron liquid closer to the interface.

IV. RESULTS AND DISCUSSION

A. Transition induced by electrostatic gating

For positive V_g (low R_N), the sheet resistance R_S goes to zero within error at low temperatures [Fig. 1(b)]. Upon decreasing V_g, the sample transitions into an anomalous metallic state with finite resistance at zero temperature [46] and then becomes insulating with $\frac{dR_S}{dT} < 0$ in the measured temperature range. As shown in Fig. 1(c), for some gate voltage $R_S(T)$ flattens at low temperatures, reaching a critical point corresponding to $R_Q = h/4e^2$. These results are similar to those of Ref. [1], where film thickness was the control parameter rather than gate voltage.

B. Transition induced by perpendicular magnetic fields

Figure 2 presents the perpendicular magnetic field (H) induced SIT in four different regimes characterized by their R_N values. For $R_N = 1.11$ kΩ the sample is superconducting at low H, and transitions into a weakly insulating state with increasing H. When R_N is increased to 5.11 kΩ, the sample is still superconducting and transitions to an insulating state under increasing H. However, R_S reaches a maximum value at some H and further increase of the field destroys this insulating behavior. For $R_N = 37.5$ kΩ, R_S remains finite at zero field, yet the field response becomes significantly stronger. Upon further increasing R_N to 96.9 kΩ the zero field $R_S(T)$ is insulating like with $\frac{dR_S}{dT} < 0$ for all temperatures [see inset of Fig. 2(g)], yet the relative amplitude of the MR peak is larger than that of the previous V_g.

H_{peak}, the field corresponding to the MR peak position, decreases with decreasing temperature (see Fig. 2), contrary to the intuition which implies the existence of a larger critical field at low temperatures. Similar results has been recently observed in InO_x [4].

Figure 1(c) shows that the zero field R_S approaches R_Q near the SIT, as expected from the self-duality between Cooper pairs and vortices in 2D superconductors [29]. However, a universal resistance value is not observed in the field induced SIT. The lack of a singular critical point in isotherms in Fig. 2 as well as the nonmonotonic behavior of $R_S(T)$ in Figs. 1(b) and 2(e) can be the result of parallel fermionic channels, similar to the results seen by Goldman *et al.* [16]. We deduce that the inhomogeneities play a less significant role at zero field from the fact that the exact quantum resistance is observed in the gate induced SIT.

Previous field driven SIT experiments have shown novel phenomena such as activated Arrhenius transport [6–8,19] and scaling behavior [2,5,15]. Arrhenius transport is the result of Cooper pair tunneling [21,47] between superconducting islands embedded in an insulating media created by self-induced inhomogeneity in uniformly disordered films [25–27,48]. The temperature dependence is characterized by an activation temperature T_A of the order of T_c [6,8]. We observed Arrhenius transport for our sample at different V_g (see the Supplemental Material for more details [37]). While the data follow the correct behavior at high temperatures similar to other experiments [6,49], the calculated T_A values are lower than T_c, implying that inter-island tunneling is not the main mechanism responsible for the insulating state. Due to the strong temperature dependence observed near the critical point, the measured resistance does not follow the expected scaling behavior, similarly to what has been seen in other materials [50] (see the Supplemental Material for more details [37]).

C. Comparison of response for different field orientations

To further understand the origin of the SIT, we performed magnetic field sweeps in parallel and perpendicular orientations (Fig. 3). The high field MR is isotropic indicating the total absence of orbital effects in the normal state (see also Ref. [51]). This important feature is contrasted with the highly anisotropic behavior at lower fields, where fluctuations can still survive. This supports the idea that the effect seen under perpendicular fields is caused by vortex excitations.

Furthermore, the MR peak is hysteretic for increasing and decreasing fields [see Figs. 3 and 4(a)]. Both positive and negative field peaks have the same resistance value when sweeping towards/away zero field. This hysteretic behavior is different from that observed in systems with magnetic order, e.g., $SrTiO_3/LaAlO_3$ nanowires [52] or other (100) interfaces [36,53]. In the vortex picture, this hysteresis is related to the effect of pinning potentials [54]. In a similar way, the glassy behavior observed in our system can be pictured as follows: When the field is swept down from higher values, the vortices move more freely, resulting in stronger dissipation and a larger resistance at the peak. In the parallel field orientation, where no field induced vortices exist, no hysteresis is observed.

D. Physical origin of the transition

Figure 4(b) shows the linear field dependence of R_S for small perpendicular H at different gate voltages. Some explanations of this behavior, such as weak localization or Maki-Thompson fluctuations, can be discounted due to their inability to account for the large amplitude and the anisotropy of the effect. This effect is very similar to flux flow, where the motion of vortices results in linear field dependent resistance. Such dependence is observed even in the highly insulating regime, implying the continued existence of mobile vortex excitations. Under these assumptions, a length scale related to the linear in field MR behavior can be estimated by $\xi_{\text{ins}} = \sqrt{\Phi_0 m/2\pi}$, where Φ_0 is the flux quantum and m is the slope of the linear MR [see Fig. 4(c)]. Despite the major difference from a standard flux-flow behavior, where the resistance drops

to zero at zero field, at the onset of the insulating regime ξ_{ins} merges quite well with the Ginzburg-Landau coherence length ξ_{GL} reported in Ref. [35]. This indicates that the quasiparticles responsible for the linear MR are of the same origin as the vortices considered in the calculation of the superconducting coherence length.

In comparison to the perpendicular field response, the response to parallel fields at low R_N starts with a flat zero resistance regime until at some field R_S increases and eventually converges with the perpendicular field curve at $H_{pairing}$. We interpret $H_{pairing}$ as the Zeeman depairing field beyond which Cooper pairs do not exist and the material becomes purely fermionic and isotropic. As R_N increases, the zero field superconductivity disappears [46] but $H_{pairing}$ can still be easily identified. The calculated values of $H_{pairing}$ are in good agreement with values observed for $SrTiO_3/LaAlO_3$ quantum dots [55] and with an estimation of the temperature for which superconducting phase order disappears (see the Supplemental Material for more information [37]) [56].

We note that $H_{pairing}$ is calculated and interpreted in a similar way to the Chandrasekhar field [57]. Yet, there are still two fundamental difference: First, $H_{pairing}$ does not describe a theoretical limit of the critical magnetic field in a superconductor but rather is the actual breakdown field of Cooper pairs. In that sense, the Clogston breakdown of a superconducting condensate [58] and the aforementioned Chandrasekhar field are identical only for a BCS-type condensate, which is certainly not our case. Second, unlike the Chandrasekhar field, $H_{pairing}$ marks the breakdown of pairing in a Bose insulator rather than a superconductor.

Finally, we note that the qualitative behavior of the MR at intermediate parallel magnetic fields is consistent with the picture of superconducting fluctuations destroyed by the field.

Figure 5 shows the R_N-H phase diagram of our interface revealing three different regimes, separated by $H_{pairing}$ and the SIT critical field $H_{critical}$. $H_{critical}$ marks the transition from the regime where condensed Cooper pairs dominate transport to an insulating phase, and gradually vanishes with increasing R_N, similar to previous SIT studies on $SrTiO_3/LaAlO_3$ interfaces [13–15]. Beyond $H_{pairing}$, the Zeeman energy exceeds the pairing one and the material transitions from a Bose insulator to a fermionic material, where no Cooper pairs exist and fermionic physics determines the transport properties. The resulting phase diagram resembles that of 2D amorphous superconductors, however, our material is a 2D crystalline heterostructure, devoid of any structural inhomogeneity or granularity, in which local disorder is screened due to the large ϵ.

Our results indicate that the intermediate insulating phase is a Bose-condensed liquid of vortex excitations, a consequence of the duality between Cooper pairs and vortices [30]. The existence of pairing in the insulating side of SITs has been confirmed from MR oscillations with $2e$ period for an array of holes in superconducting film [19,21,47] and the presence of a superconducting gap [48,59]. The observed large MR peak is another signatures of such Bose insulator [5–9,21].

While the magnetic field induced SIT has been reported for the (100) and (110) interfaces [13–15], a clear MR peak was not observed and the nature of insulating regime has not been investigated. We speculate that the more extreme SIT

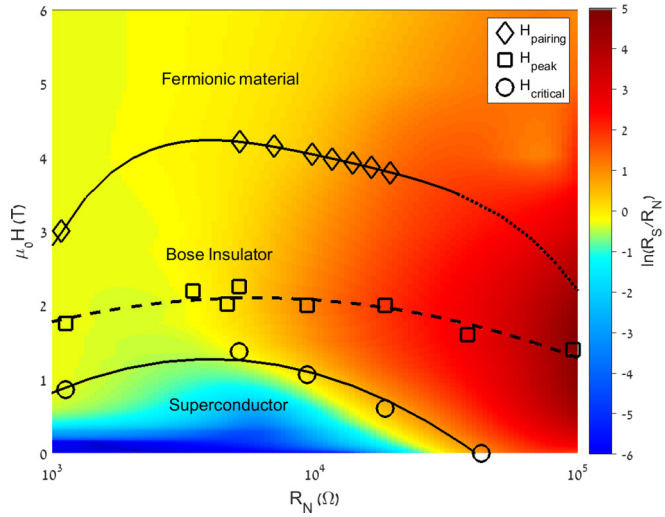

FIG. 5. $\ln(R_S/R_N)$ at 35 mK plotted against R_N and H. The SIT critical field $H_{critical}$ defined as the field for which $\frac{dR_S}{dT}_{T\to 0} = 0$, the field corresponding to the maximum of the MR peak H_{peak} and the depairing field $H_{pairing}$ are also plotted (see the Supplemental Material for more details [37]). The solid black lines (guide to the eye) show the borders between different states: the superconducting region below $H_{critical}$, the Bose insulator between $H_{critical}$ and $H_{pairing}$, and the Fermionic material beyond $H_{pairing}$. The dotted part of top line shows the extrapolated border of $H_{pairing}$ for higher R_N. The dashed line marks the boundary where the effect of the field on R_S changes direction.

observed in the (111) interface compared to the (100) and (110) cases may be related to frustrated antiferromagnetic coupling in the (111) triangular interface, which allows superconductivity to exist in a broader R_N region. Such antiferromagnetic coupling has been observed in (100) $SrTiO_3/LaAlO_3$ nanowires [52]. Previous work on (100) $SrTiO_3/LaAlO_3$ showed that charge-vortex duality is related to the SIT [36], where a change in the MR with field sweep rate was caused by the interplay of ferromagnetism and superconductivity. The indifference of the MR on sweep rate in our case hints that the magnetic response of the (111) interface plays a less significant role.

E. Zero field bosonic insulator

One of the more striking features observed in Fig. 5 is the existence of a Bose-insulator state at zero field. For example, at $R_N = 96.9$ kΩ [Figs. 2(g) and 2(h)] the sample is insulating even at zero field and yet this anomalous insulating state exhibits *the same* MR peak observed when the sample is superconducting. While the peak in the MR has been previously shown to be related to the SIT in amorphous superconductors [5–9], in these experiments the different regimes could only be accessed in different samples. In our measurements, the continuous evolution of the MR peak with increasing R_N shows that even in the zero-field insulating state, the mechanism responsible for the SIT still effects the transport properties of the system. At zero field the insulating state cannot be ascribed to the condensation of vortices but rather the condensation of vortex fluctuations, resulting in a

zero-field Bose insulator. While previous works have shown the existence of intrinsically insulating states [60] or Cooper pairs in an insulating state [21,21,47], our results allow us to track the evolution of the SIT features down from the superconducting regime to the insulating one.

V. SUMMARY

We study the superconductor-to-insulator transition in a (111) $SrTiO_3/LaAlO_3$ interface. The quantum phase transition is controlled by gate voltage and magnetic field. The tunability of our system allows us to follow features related to the superconductor-to-insulator transition such as the magnetoresistance peak and the various critical fields deep into the insulating state. We observe a gate-controlled transition from the superconducting to the insulating state at the quantum resistance similar to the hallmark data of Haviland, Liu, and Goldman [1], indicating the importance of duality in the transition. We use the comparison of measurements in parallel and perpendicular field to define and follow a new energy scale related to the depairing field H_{pairing}. The linear field dependence of the magnetoresistance at low fields and the resulting length scale, the strong anisotropy of the magnetoresistance at the peak region, and the hysteresis of the peak all are evidence that this peak is related to the formation of a liquid of vortex excitations. Our data present the continuous evolution of a variety of phenomena observed, until now, in many different samples and regimes and show that vortices play an important role in the insulating state observed beyond the superconductor-to-insulator transition in this material. Finally, we show that in the regime of very negative gate voltages, where superconductivity is completely suppressed, there exists a Bose-insulating state even at zero magnetic fields.

ACKNOWLEDGMENTS

We are indebted to Aharon Kapitulnik, Dan Shahar, Moshe Goldstein, Alexander Palevski, Efrat Shimshoni, Tsofar Maniv, Igor Bormistrov, Pratap Raychaudhuri, Amnon Aharoni, Ora Entin-Wohlman, Giancarlo Strinati, Guy Deutscher, Tal Levinson, Adam Doron, and Idan Tamir for useful discussions. This work has been supported by the Israel Science Foundation under Grant No. 382/17 and the Bi-national science foundation under Grant No. 2014047. A portion of this work was performed at the National High Magnetic Field Laboratory, which is supported by National Science Foundation Cooperative Agreement No. DMR-1157490 and the State of Florida.

[1] D. B. Haviland, Y. Liu, and A. M. Goldman, Phys. Rev. Lett. **62**, 2180 (1989).
[2] A. F. Hebard and M. A. Paalanen, Phys. Rev. Lett. **65**, 927 (1990).
[3] M. Ovadia, D. Kalok, B. Sacépé, and D. Shahar, Nat. Phys. **9**, 415 (2013).
[4] A. Doron, I. Tamir, T. Levinson, F. Gorniaczyk, and D. Shahar, Phys. Rev. B **98**, 184515 (2018).
[5] M. A. Steiner, N. P. Breznay, and A. Kapitulnik, Phys. Rev. B **77**, 212501 (2008).
[6] G. Sambandamurthy, L. W. Engel, A. Johansson, and D. Shahar, Phys. Rev. Lett. **92**, 107005 (2004).
[7] M. A. Steiner, G. Boebinger, and A. Kapitulnik, Phys. Rev. Lett. **94**, 107008 (2005).
[8] T. I. Baturina, A. Y. Mironov, V. M. Vinokur, M. R. Baklanov, and C. Strunk, Phys. Rev. Lett. **99**, 257003 (2007).
[9] T. I. Baturina, C. Strunk, M. R. Baklanov, and A. Satta, Phys. Rev. Lett. **98**, 127003 (2007).
[10] A. Yazdani and A. Kapitulnik, Phys. Rev. Lett. **74**, 3037 (1995).
[11] X. Leng, J. Garcia-Barriocanal, S. Bose, Y. Lee, and A. M. Goldman, Phys. Rev. Lett. **107**, 027001 (2011).
[12] A. T. Bollinger, G. Dubuis, J. Yoon, D. Pavuna, J. Misewich, and I. Božović, Nature (London) **472**, 458 (2011).
[13] J. Biscaras, N. Bergeal, S. Hurand, C. Feuillet-Palma, A. Rastogi, R. C. Budhani, M. Grilli, S. Caprara, and J. Lesueur, Nat. Mater. **12**, 542 (2013).
[14] S. Shen, Y. Xing, P. Wang, H. Liu, H. Fu, Y. Zhang, L. He, X. C. Xie, X. Lin, J. Nie *et al.*, Phys. Rev. B **94**, 144517 (2016).
[15] M. M. Mehta, D. A. Dikin, C. W. Bark, S. Ryu, C. M. Folkman, C. B. Eom, and V. Chandrasekhar, Phys. Rev. B **90**, 100506 (2014).
[16] H. M. Jaeger, D. B. Haviland, B. G. Orr, and A. M. Goldman, Phys. Rev. B **40**, 182 (1989).
[17] Y. Qin, C. L. Vicente, and J. Yoon, Phys. Rev. B **73**, 100505 (2006).
[18] H. Aubin, C. A. Marrache-Kikuchi, A. Pourret, K. Behnia, L. Bergé, L. Dumoulin, and J. Lesueur, Phys. Rev. B **73**, 094521 (2006).
[19] M. D. Stewart, A. Yin, J. M. Xu, and J. M. Valles, Science **318**, 1273 (2007).
[20] A. E. White, R. C. Dynes, and J. P. Garno, Phys. Rev. B **33**, 3549 (1986).
[21] H. Q. Nguyen, S. M. Hollen, M. D. Stewart, J. Shainline, A. Yin, J. M. Xu, and J. M. Valles, Phys. Rev. Lett. **103**, 157001 (2009).
[22] A. Finkel'stein, Physica B: Condens. Matter **197**, 636 (1994).
[23] I. S. Burmistrov, I. V. Gornyi, and A. D. Mirlin, Phys. Rev. B **92**, 014506 (2015).
[24] P. Szabó, T. Samuely, V. Hašková, J. Kačmarčík, M. Žemlička, M. Grajcar, J. G. Rodrigo, and P. Samuely, Phys. Rev. B **93**, 014505 (2016).
[25] E. Shimshoni, A. Auerbach, and A. Kapitulnik, Phys. Rev. Lett. **80**, 3352 (1998).
[26] Y. Dubi, Y. Meir, and Y. Avishai, Nature (London) **449**, 876 (2007).
[27] M. A. Skvortsov and M. V. Feigel'man, Phys. Rev. Lett. **95**, 057002 (2005).
[28] V. F. Gantmakher and V. T. Dolgopolov, Phys.-Usp. **53**, 1 (2010).
[29] M. P. A. Fisher, G. Grinstein, and S. M. Girvin, Phys. Rev. Lett. **64**, 587 (1990).
[30] M. P. A. Fisher, Phys. Rev. Lett. **65**, 923 (1990).

[31] G. Herranz, F. Sánchez, N. Dix, M. Scigaj, and J. Fontcuberta, Sci. Rep. **2**, 758 (2012).
[32] P. K. Rout, I. Agireen, E. Maniv, M. Goldstein, and Y. Dagan, Phys. Rev. B **95**, 241107 (2017).
[33] A. Monteiro, A. M. R. V. L. Monteiro, D. J. Groenendijk, I. Groen, J. de Bruijckere, R. Gaudenzi, H. S. J. van der Zant, and A. D. Caviglia, Phys. Rev. B **96**, 020504(R) (2017).
[34] S. Davis, Z. Huang, K. Han, Ariando, T. Venkatesan, and V. Chandrasekhar, Phys. Rev. B **96**, 134502 (2017).
[35] P. K. Rout, E. Maniv, and Y. Dagan, Phys. Rev. Lett. **119**, 237002 (2017).
[36] M. M. Mehta, D. A. Dikin, C. W. Bark, S. Ryu, C. M. Folkman, C. B. Eom, and V. Chandrasekhar, Nat. Commun. **3**, 955 (2012).
[37] See Supplemental Material at http://link.aps.org/supplemental/10.1103/PhysRevB.99.094507 for more details about sample fabrication and characterization, measurements conducted for multiple samples, the difference in gate response in separate cool downs, Arrhenius analysis, scaling analysis, Emery-Kivelson calculation, and the calculation of the critical fields.
[38] A. Caviglia, S. Gariglio, N. Reyren, D. Jaccard, T. Schneider, M. Gabay, S. Thiel, G. Hammerl, J. Mannhart, and J.-M. Triscone, Nature (London) **456**, 624 (2008).
[39] B. Kalisky, E. M. Spanton, H. Noad, J. R. Kirtley, K. C. Nowack, C. Bell, H. K. Sato, M. Hosoda, Y. Xie, Y. Hikita *et al.*, Nat. Mater. **12**, 1091 (2013).
[40] M. Honig, J. A. Sulpizio, J. Drori, A. Joshua, E. Zeldov, and S. Ilani, Nat. Mater. **12**, 1112 (2013).
[41] J. Biscaras, S. Hurand, C. Feuillet-Palma, A. Rastogi, R. C. Budhani, N. Reyren, E. Lesne, J. Lesueur, and N. Bergeal, Sci. Rep. **4**, 6788 (2014).
[42] S. Davis, V. Chandrasekhar, Z. Huang, K. Han, Ariando, and T. Venkatesan, Phys. Rev. B **95**, 035127 (2017).
[43] U. Khanna, P. K. Rout, M. Mograbi, G. Tuvia, I. Leermakers, U. Zeitler, Y. Dagan, and M. Goldstein, arXiv:1901.10931.
[44] E. Maniv, M. Ben Shalom, A. Ron, M. Mograbi, A. Palevski, M. Goldstein, and Y. Dagan, Nat. Commun. **6**, 8239 (2015).
[45] C. Bell, S. Harashima, Y. Kozuka, M. Kim, B. G. Kim, Y. Hikita, and H. Y. Hwang, Phys. Rev. Lett. **103**, 226802 (2009).
[46] A. Kapitulnik, S. A. Kivelson, and B. Spivak, Rev. Mod. Phys. **91**, 011002 (2019).
[47] G. Kopnov, O. Cohen, M. Ovadia, K. H. Lee, C. C. Wong, and D. Shahar, Phys. Rev. Lett. **109**, 167002 (2012).
[48] B. Sacépé, T. Dubouchet, C. Chapelier, M. Sanquer, M. Ovadia, D. Shahar, M. Feigel'man, and L. Ioffe, Nat. Phys. **7**, 239 (2011).
[49] M. Steiner and A. Kapitulnik, Physica C: Superconduct. **422**, 16 (2005).
[50] V. F. Gantmakher, M. V. Golubkov, V. T. Dolgopolov, G. E. Tsydynzhapov, and A. A. Shashkin, J. Exp. Theor. Phys. Lett. **71**, 160 (2000).
[51] M. Ben Shalom, C. W. Tai, Y. Lereah, M. Sachs, E. Levy, D. Rakhmilevitch, A. Palevski, and Y. Dagan, Phys. Rev. B **80**, 140403 (2009).
[52] A. Ron, E. Maniv, D. Graf, J.-H. Park, and Y. Dagan, Phys. Rev. Lett. **113**, 216801 (2014).
[53] A. Brinkman, M. Huijben, M. Van Zalk, J. Huijben, U. Zeitler, J. Maan, W. Van der Wiel, G. Rijnders, D. Blank, and H. Hilgenkamp, Nat. Mater. **6**, 493 (2007).
[54] M. Marziali Bermúdez, E. R. Louden, M. R. Eskildsen, C. D. Dewhurst, V. Bekeris, and G. Pasquini, Phys. Rev. B **95**, 104505 (2017).
[55] G. Cheng, M. Tomczyk, S. Lu, J. P. Veazey, M. Huang, P. Irvin, S. Ryu, H. Lee, C.-B. Eom, C. S. Hellberg *et al.*, Nature (London) **521**, 196 (2015).
[56] V. J. Emery and S. A. Kivelson, Nature (London) **374**, 434 (1995).
[57] B. Chandrasekhar, Appl. Phys. Lett. **1**, 7 (1962).
[58] A. M. Clogston, Phys. Rev. Lett. **9**, 266 (1962).
[59] D. Sherman, G. Kopnov, D. Shahar, and A. Frydman, Phys. Rev. Lett. **108**, 177006 (2012).
[60] B. Sacépé, J. Seidemann, M. Ovadia, I. Tamir, D. Shahar, C. Chapelier, C. Strunk, and B. A. Piot, Phys. Rev. B **91**, 220508 (2015).